UNIVERSITY OF CALIFORNIA SAN DIEGO

Spatiotemporal Ribosome Allocation in *Escherichia Coli*

A Thesis submitted in partial satisfaction of the
requirements for the degree Master of Science

in

Biology

by

Chun Chan

Committee in charge:

Professor Lin Chao, Chair
Professor Justin Meyer, Co-chair
Professor Ronald Burton

2022

The thesis of Chun Chan is approved, and it is acceptable in quality and form for publication on microfilm and electronically.

University of California San Diego

2022

TABLE OF CONTENTS

LIST OF FIGURES

ACKNOWLEDGMENTS

I would like to first acknowledge Professor Lin Chao for his support as the chair of my committee. Through his extensive mentorship and passion on biological research, I gained immense amounts of knowledge in this field, as well as life-long benefits of being a better problem solver.

I also want to thank my committee members: Professor Justin Meyer and Professor Ronald Burton, for their time and support in my journey of being a scientist.

I would like to thank my colleagues, Ulla Camilla Rang and Chao Shi, without whom I would not have been able to accomplish what I can today.

This thesis, in part, is currently being prepared for submission for publication of the material: Chao, Lin; Chan, Chun (first co-author); Shi, Chao; Rang, Ulla Camilla. "Spatiotemporal Allocation of Ribosomes to Daughter Cells is Determined by the Age of the Mother in Single *Escherichia coli*" *In preparation*. The thesis author was the primary investigator and author of this material.

ABSTRACT OF THE THESIS

Spatiotemporal Ribosome Allocation in *Escherichia Coli*

by

Chun Chan

Master of Science in Biology

University of California San Diego, 2022

Professor Lin Chao, Chair
Professor Justin Meyer, Co-chair

Variations in growth rate for *Escherichia coli* were partly explained by the mother's asymmetrical partitioning of damage and expressed gene products to its daughters. Between a daughter pair, the old daughter receives more damage and fewer expressed gene products,

resulting in slower growth and thus said to be aging. Because ribosomes serve as cellular protein factories and are positively correlated with growth rate, it was hypothesized that ribosomes could also be allocated asymmetrically. By following cells with yfp-labeled ribosomes under time-lapse microscopy, we found that new daughters overall had a higher level of ribosomes than did old daughters, and the stronger asymmetry was associated with daughter pairs from old mothers. Moreover, we found the ribosome concentration to be higher at the old pole at birth and thereafter successively decreasing at the old pole and partly becoming redistributed to the mid-section as the cell elongates. At the time of division, ribosomes, at pinching site where the two new poles are being produced, were unevenly distributed, which was then associated with a higher ribosomal content in the new daughter and positively correlated with higher growth rate.

INTRODUCTION

Ribosomes in *Escherichia coli* are highly unevenly distributed within the cell and anti-correlates spatially with the condensed DNA (nucleoid), both shifting their distribution temporally with the cell cycle. The nucleoid, consisting of condensed DNA and DNA-associated proteins, obstructs the diffusion of ribosomes and physically compartmentalizes them into different regions that are DNA free, such as the poles. As the cell elongates and prepares to divide at mid-plane, the DNA duplicates and shifts position from one copy in the center to one copy each at the two outer quarter points. Simultaneously, the ribosomes also adjust their spatial concentration from the two poles to additionally congregate in the center of the cell so that the two daughters at the time of division contain ribosomes at both of its poles [1–3]. Our imaging analysis using fluorescently labeled ribosomes confirmed the above ribosomal fluent findings (Figure 2). However, we noted that one end of a cell had higher ribosomal fluorescence than the other.

E. coli is a rod-shaped bacterium that divides at the mid-plane of its long axis, forming two new poles at the middle. Therefore, each resulting daughter cell has a new pole facing each other, and an old pole at the distal end (Figure 1). When a mother cell divides, one of its daughters that receives the maternal old pole is denoted as old daughter, and the other receiving the maternal new pole as new daughter. However, note that when the polarity of the first cell is unknown, assignment of old and new poles can be achieved after one division, but two divisions are required to determine old and new daughters (Figure 1). Previous studies have shown that new and old daughters have different growth rates, favoring the new daughter [4–13]. A recent study reported higher levels of expressed proteins in new daughters than old daughters, and highly significantly so when the daughters were born from an old mother. An old daughter from

an old mother also had a significant internal spatial asymmetry between its old and new pole, with higher levels of proteins at the new pole [14].

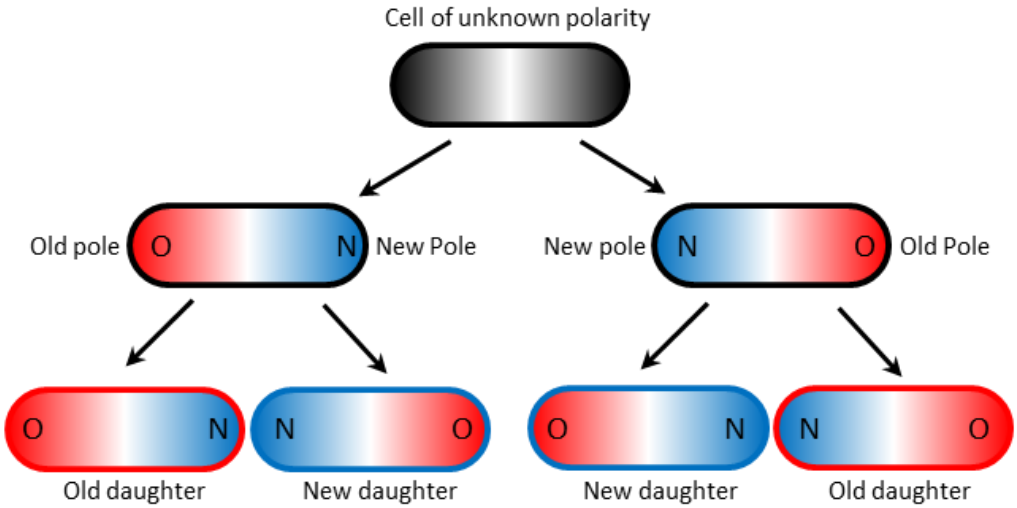

Figure 1. Assignment of old and new pole and daughters in E. coli. The outlines of cells in this figure are colored black, red and blue to designate them as cells with unknown genealogy, old and new daughters. The intracellular spaces of cells are colored red and blue to identify the old and new pole, also denoted as O and N.

Because ribosomes function as the cells' protein factories, and the number of ribosomes and growth rate are positively correlated [15–18], we explored whether the allocation and/or internal spatial distribution of ribosomes followed the same aging pattern as above with an asymmetry between old and new daughters and poles. We found that new daughters overall had a higher level of ribosomes than did old daughters, and, as with protein levels, the asymmetrical signal was the strongest when the daughters came from an old mother. Moreover, we found the ribosome concentration to be higher at the old pole at birth (just after division) and thereafter successively decreasing at the old pole and partly becoming redistributed to the mid-section as the cell becomes longer, to eventually end up and increase at the pinching site where the two new poles are being produced. This was then associated with a higher ribosomal content in the new

daughter and positively correlated with higher growth rate. As stated and modeled in earlier studies, a variation in growth rates between kin-cells has an evolutionary advantage because it increases the efficiency of selection [9]. It is most interesting to notice that what in earlier days was reported as pure stochasticity in symmetrically dividing bacteria, has in the last decade been shown to largely consist of a deterministic component in line with an early evolutionary stage of aging [5, 12, 14, 19–22] .

MATERIALS AND METHODS

Bacterial strains and growth media

Growth experiments were performed using *E. coli* AFS55, containing a translational fusion of *yfp* to the C-terminus of rpsB (the gene coding for the ribosomal subunit S2) [3], used as a reporter to quantify ribosomal levels. The strain was kindly provided by Dr. Weisshaar, University of Wisconsin-Madison. Cells were grown in M9 minimal media [25] supplemented with 0.02 mg ml^{-1} of thiamine and 2 mg ml^{-1} glucose.

Bacterial growth and microscope slides

Cells from -80° C glycerol stock were streaked onto agar plates. After growth into colonies, a single colony was inoculated into M9 media and incubated at 37° C overnight. The culture was diluted at 1:100 in M9 in the following day and grew for 2 hours. 1 µl of the 2-hour culture was then pipetted onto a 10 µl M9 15% agarose pad with the thickness of a No. 1 coverslip. The agarose pad was then flipped with the bacterial side down onto a 24 x 60 mm cover glass and placed over a 25 x 75 mm single depression slide sealed with Vaseline to fit an inverted microscope. Individual cell from two different time-lapse movies was followed under the microscope, growing at 37° C until micro-colonies of at least 64 cells were reached.

Time-lapse microscopy

Cells were imaged with an inverted microscope (Nikon Eclipse Ti-S), equipped with Nikon NIS-Elements AT control software, 100X objective (CFI Plan APO NA 1.4) external phase contrast rings for full intensity fluorescence imaging (FITC) fluorescence light source (Prior Lumen 200) with motorized shutter (Lambda 10-B Sutter SmartShutter) and camera

(Retiga 2000R FAST 1394 mono, 12 bit). Phase contrast and fluorescence images were recorded every 2 and 20 mins, respectively.

Image quantification and analysis

The software ImageJ (NIH) was used to manually trace cell outlines on the phase contrast images and subtract the background of each fluorescent frame with cell tracings, using 'rolling ball' algorithm with ball radius 20 pixels. Noise created by heat overflow of single pixel was corrected by 'remove outliers' algorithm in ImageJ with threshold intensity difference 1000 and threshold radius 0.5 pixel. To correct for diffractional scatter of fluorescence from a cell to its neighbor within a colony, images were deconvoluted by the Lucy-Richardson method in Matlab 2017b (The MathWorks, Inc., Natick, MA) (see [14] for details). The cell outlines were then transferred, along with the corresponding fluorescence frame, into R-programming for quantifying density of fluorescence for each cell. In addition, R-programming was used to find the accurate cellular cut-offs to split a cell in half for differential polar measurements. Moreover, a transect, which spans through the long axis of a cell, was used as a vector to store fluorescence measurements serving as a ribosomal distribution profile for that cell.

Time quartiles of cell cycle

To record the spatial fluency of the ribosomal content during growth, the individual cell life cycle, regarded as a time window, was divided into four stages: birth, second quartile (2ndQ), third quartile (3rdQ), and division. That time window was first manually recorded for each cell from phase images (ImageJ). Then, in each fluorescence image, each cell was assigned a life percentage using the time when that image was taken divided by the time window of cell cycle

for that cell. A life percentage between 0 to 25 percent belongs to the first cell cycle quartile of birth; 25 to 50 percent to SecQ, and so forth. In other words, birth quartile represents cells that are just created from mothers' division, while division quartile represents cells that are preparing for the act of dividing into two daughters.

Normalization of transect fluorescence and length

A transect of a cell is a vector storing fluorescence measurements, serving as a representative ribosomal profile. Because fluorescence images were taken every 20 minutes, the recorded cells were in different stages of life cycle and thus lengths of transect vectors were different. In order to pool the transect vectors and account for the different lengths in comparison analysis, transect vectors were stretched into the maximum length of all cells, with fluorescence measurements equally distributed. Then, we divided each fluorescence value by the sum of all measurements in that transect vector. Lastly, these pooled normalized transect vectors were binned into quartiles, or eight parts depending on the analysis. For example, in the case with quartile bins, the first 25 percent of the measurements on a transect vector will be put into the first bin, and the next 25 percent to the second bin, and so forth. The sum of measurements at each bin was divided by the total number of pooled cells, which will be used to construct normalized ribosomal profile for the average population. Note that each normalized transect will have a sum of 1.

Elongation rate measurement

Fluorescence measurements for pairs of old and new daughters were normalized by subtracting the mean of the pair's value and subsequently divided by the mean. Elongation rates

were calculated as follows: lengths of individual bacterial cells were extracted manually from time-lapse images (ImageJ). From lengths compiled over time, the elongation rate *r* was estimated as the slope of a linear regression of (log/length) over time. Because elongation rates are known to be exponential [4], a log transformation was used. Lengths were measured immediately after division and prior to the next division.

Statistical analysis

All statistical analysis was performed in the software R. Analysis of ratios were done with *t*-tests. Choices of paired, unpaired, one- or two-tailed comparisons are provided in the figure legends (Figure3). For trend lines in Figure 4, a linear regression model was fit at each bin with the four normalized fluorescence values associated with time quartiles. Two-way ANOVA was used to compare transects, followed by post-hoc test to reveal bins with significant difference (Figure 5). Randomized designs were used when data did not conform to standard Gaussian requirements (Figure 6). Sample sizes, p values, and choice of statistical test were provided in the figure legends. Values are presented as mean ± s.e.m. (standard error of the mean) when appropriate. Significant level is shown as * for $p < 0.05$, ** for $p < 0.01$, and *** for $p < 0.001$.

RESULTS

Spatial dynamics of ribosome concentrations during cell's life cycle

To confirm earlier studies of fluent ribosome concentrations in *E. coli*'s different stages of life cycle following a specific pattern [3], we followed single cell growth under the microscope of *E. coli* AFS55 with time lapse fluorescent images. Fluorescence was analyzed as whole cell intracellular "heatmaps" from birth to division. Our results confirmed the same pattern as previously described by Bakshi et al [3], with high ribosomal concentrations by the poles in a cell's early life stage, and slowly building up additionally in the middle of the cell as the bacteria elongates, to be at the mid-plane maximum when approaching division. Representative images of daughter cells at the time of birth and division are shown in Figure 2. At birth, ribosomes are concentrated mainly at the poles (Figure 2 c2 & c4). At division, high concentration of ribosomes is also clustered at the mid-section of the cell (Figure 2 c3). In addition to the same pattern observed as previously published, we noticed that ribosome concentrations were different between the poles of a cell and between daughter pairs, suggesting an asymmetrical pattern similar to our recent findings on expressed gene products [14].

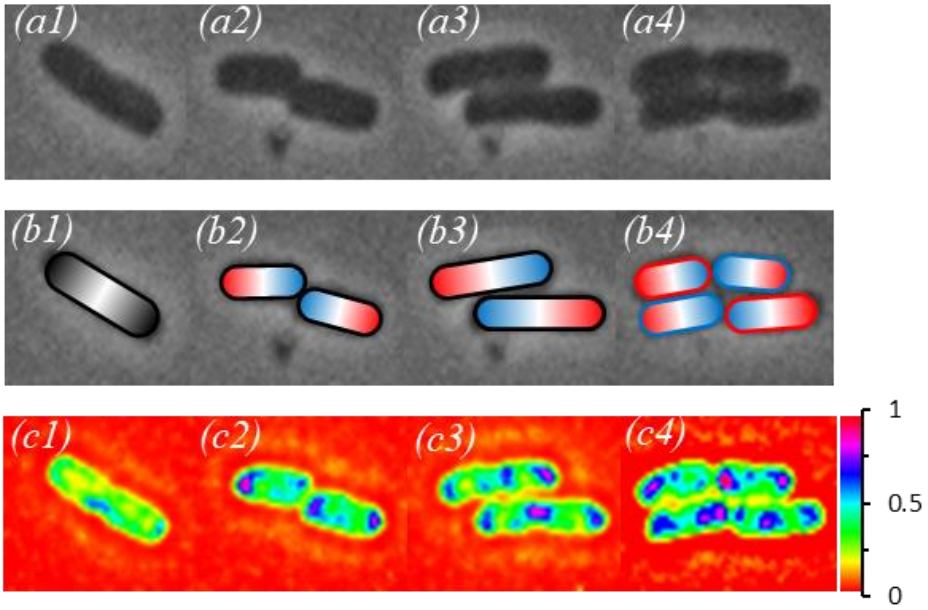

Figure 2. Time-lapse microscopy images of an E. coli bacterium dividing into two and four cells. Row a: Phase contrast, showing a cell with unknown polarity (a1), two cells at birth (a2), the same two cells at division (a3), their four daughters at birth (a4). Row b: Assignment of old (red) and new (blue) poles and daughters from the top row cells, following the method provided in figure 1. Row c: Heat-map of fluorescent images of row a cells. Scale on the right indicates levels of intensity: highest = pink, lowest = orange.

Ribosome levels are biased towards new daughters at birth, and additionally at the new poles at division

To investigate whether an asymmetry in ribosome levels between daughter cells exists, we first analyzed the level of yellow fluorescent protein (YFP) between new and old daughter pairs descending from the same mother at birth. The average fluorescent ratio between new and old daughters was 1.08 ± 0.012 ($p = 4.38 \times 10^{-6}$), indicating new daughters on average contain more ribosomes. However, when dividing the daughter pairs further into whether they originate from new or old mothers, a significant difference was seen between the two groups ($p = 0.007$). When the daughters originated from a new mother, the ratio was 1.04 ± 0.015 ($p = 0.04$), while the ratio was 1.11 ± 0.018 ($p = 6.89 \times 10^{-6}$) if they were born from an old mother (Figure 3a).

Both ratios appeared to be larger than 1; however, significance associated with ratios from daughters of old mothers was much stronger and the corresponding ratio was much greater than 1, indicating a larger asymmetry between the daughters from old mothers than from new mothers.

To further explore whether this ribosomal asymmetrical pattern between the daughters was already present in their mothers, we compared florescence at the new and old pole of respective daughters' mothers at division. The samples were analyzed as trios: a mother cell versus old and new daughters respectively. We found that new poles in the mother cells were brighter than the old poles with average pole ratios (new/old) of 1.03 ± 0.010 ($p = 0.08$) in new mothers and 1.10 ± 0.015 ($p = 6.23 \times 10^{-5}$) in old mothers (figure 3b). The difference between these two groups of pole ratios was significant ($p = 1.3 \times 10^{-4}$). Following the same pattern observed above, pole ratios from old mothers was significantly larger than 1, which suggests the asymmetry between the poles was stronger in old mothers. To confirm if the ribosomal asymmetry in the mother at division translated into their daughters at birth, the pole ratios in the mothers were then compared to corresponding daughter ratios, and no significant difference was observed in neither new nor old trios ($p = 0.27$ and 0.62, respectively).

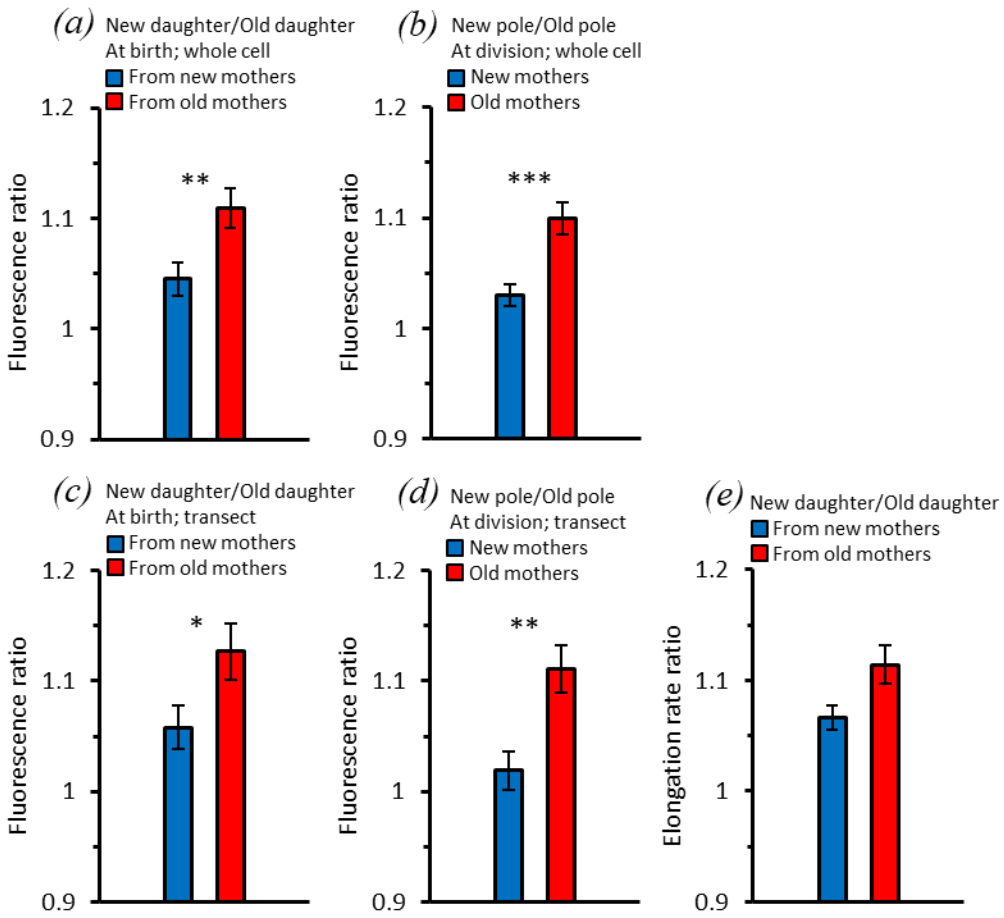

Figure 3. Ratios of fluorescence and elongation rate within and between cells. (a) Daughter (new/old) ratios at birth. Daughter ratio from old mothers is 1.11 ± 0.018 ($p = 6.89 \times 10^{-6}$, one-tailed paired t-test, n = 89 pairs) and from new mothers 1.04 ± 0.015 (p = 0.04, one-tailed paired t-test, n = 91 pairs). The difference between the two ratios is significant (p= 0.007, two-tailed non-paired t-test). (b) Pole (new/old) ratio in mothers at division. Asymmetry between the two polar halves in old mothers is higher with a 1.10 ± 0.015 ($p = 6.23 \times 10^{-5}$, one-tailed paired t-test, n = 89 pairs) than 1.03 ± 0.010 (p = 0.08, one-tailed paired t-test, n = 91 pairs in new mothers. The difference between the two ratios is significant ($p= 1.3 \times 10^{-4}$, two-tailed non-paired t-test). (c) Daughter (new/old) ratios at birth based on transects. The ratio of daughters from old mothers is 1.13 ± 0.026 ($p = 3.15 \times 10^{-5}$, one-tailed paired t-test, n = 89 pairs) and from new mothers 1.06±0.020 (p = 0.013, one-tailed paired t-test, n = 91 pairs). The difference between the two ratios is significant (p= 0.036, two-tailed non-paired t-test). (d) Pole (new/old) ratio in mothers at division based on transects. The ratio for old mothers is 1.11 ± 0.022 ($p = 6.85 \times 10^{-6}$, one-tailed paired t-test, n = 89 pairs) and new mother 1.02 ± 0.017 (p = 0.33, one-tailed paired t-test, n = 91 pairs). The difference between the two ratios is significant (p= 0.001, two-tailed non-paired t-test). (c) Elongation rate (new/old) ratios. The ratio from old mothers is 1.11 ±0 .017 ($p = 1.3 \times 10^{-10}$, one-tailed paired t-test, n = 216 pairs) and from new mothers 1.07±0.011 ($p = 2.76 \times 10^{-7}$, one-tailed paired t-test, n = 198 pairs). The two ratios are significantly different from each other (p= 0.02, one-tailed non-paired t-test).

Florescent density along transect preserves the same characteristics as density of the poles and entire cells.

Because ribosomes are segregated by the nucleoid, they are located predominately at the two ends of a short cell, and additionally the middle region of an elongated cell later in its life cycle. A transect, a vector storing fluorescence measurements along the long axis of a cell, could therefore be used as a representative ribosomal profile for a cell, which will allow us to observe changes in a finer resolution. To confirm the viability of transect data, we looked at the pole and daughter ratios based on transect to discover whether the asymmetrical properties could still be reflected.

Cell lengths and fluorescence of transects were normalized (see Materials and Methods). Similar to the whole cell fluorescence finding above, the transect results show that a daughter ratio of 1.06 ± 0.020 ($p = 0.013$) was obtained from comparing daughter pairs of new mothers and 1.13 ± 0.026 ($p = 3.15 \times 10^{-5}$) from daughters of old mothers (Figure 3c). Furthermore, new poles from both new and old mothers were brighter with pole ratios of 1.02 ± 0.017 ($p = 0.33$) and 1.11 ± 0.022 ($p = 6.85 \times 10^{-6}$), respectively (Figure 3d). Stronger asymmetry was associated with old mother linage with both pole ratio and daughter ratio being significantly larger than 1, and the two ratios matches each other closely ($p = 0.53$). In the new mother linage, although daughter ratio was significantly larger than 1 whereas pole ratio was not, the two distributions of ratios were not significantly different from each other ($p = 0.07$), and thus, we can safely conclude that the weaker asymmetrical pattern in pole ratio of new mothers at division also translates into their daughters at birth. Analysis using florescent density along transect closely replicated the asymmetrical trends presented in analysis using whole cell fluorescence of the poles and entire cells.

Shuffling of ribosomes from old pole to mid-section within generation throughout cell cycle

Since the asymmetrical pattern between poles of mother cells at division were translated to their daughters at birth, we wanted to find out if that pattern was present in mother cells at birth and how it changed throughout cell cycle to become asymmetrical at division. Because transects were viable for analysis, we followed mother cells of the trios from birth to division to observe changes in ribosomal presence along the transect during growth. The cells were normalized for length and density fluorescence, which was binned at the four quartiles along the cell length. The cells were analyzed in the four life cycle stages of Birth, SecQ, ThirdQ and Division (see Materials and Methods for details).

We found that both new and old mothers experienced a significant decrease ($p = 0.001$ and 0.005, respectively) in ribosomal concentration at the last bin, the old pole, from birth to division (Figure 4). The decrease at the old pole was accompanied by increases at the middle two bins as the cells went through its life cycle. Interestingly, the magnitudes of increases between the two bins were different in the two mothers. In old mothers, significant increase was found at the second bin ($p = 0.007$) with a slope of 0.0169 whereas a shallower slope of 0.009 for the third bin was not significant ($p = 0.056$) (Figure 4a). In new mothers, significant increases were associated with both second and third bin ($p = 0.025$ and 0.022) with similar slopes of 0.0191 and 0.013 (Figure 4b). Slopes of the second bins in both mothers appeared to be larger than those of the third bins, which indicates the gain of ribosomal density at the mid-section was most drastic at the area where the new pole for the new daughter will be produced. Furthermore, this effect was more pronounced in old mothers, which was consistent with a higher asymmetry between the poles of old mothers at division favoring the new half (Figure 3b).

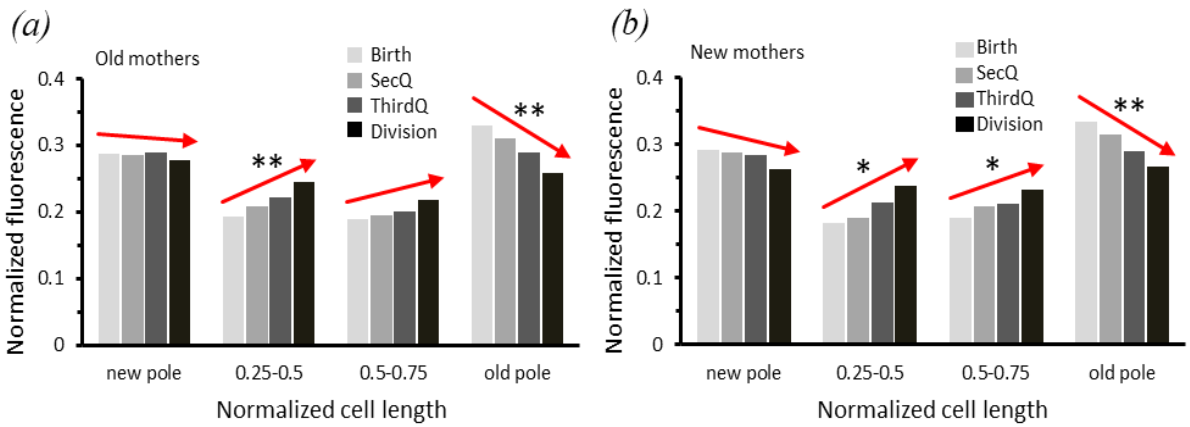

Figure 4. Fluorescence distributions along transect in mothers of trios followed from birth to division. (a) Fluorescence changes in the life cycle of old mothers (n = 71, 74, 46, 89 cells, respectively for Birth, SecQ, ThirdQ, Division). Slopes for trend lines are -0.0028 (p = 0.32), 0.0169 (p = 0.007), 0.009 (p = 0.056) and -0.023 (p = 0.005), respectively from new to old pole. (b) Fluorescence changes in the life cycle of new mothers (n = 68, 72, 49, 91 cells, respectively for Birth, SecQ, ThirdQ, Division). Slopes for trend lines are -0.0091 (p = 0.082), 0.0191 (p = 0.025), 0.013 (p = 0.022) and -0.023 (p = 0.001), respectively from new to old pole.

A complete cycle in dynamics of ribosome distribution within and across generation

By following mother cells from birth to division, ribosomes were shown to be shuffled from old pole to mid-section of the cell (Figure 4) with a construction of asymmetry favoring new half of the mothers at division. Previously, we found that this asymmetry in the poles of mothers at division was translated into their daughters at birth (Figure 3), in terms of a big picture with ratios. Therefore, we wanted to discover whether there would be any difference in analysis with a finer resolution using transects. This would essentially summarize the dynamics of ribosomal distribution in the life of *E. coli*, as a cycle from birth to division of mother cells and to their daughters at birth.

Transects of mothers at birth were first shown with a normalized transect length of 4 bins (Figure 5a & 5e), which were the same distributions as those for birth in Figure 4. Then, they were renormalized to a length of 8 bins (Figure 5b & 5f) for comparison with the 8-bin transects

of mothers at division to observe florescence changes at more precise locations. From birth to division, both new and old mothers experienced a significant decrease in normalized florescence at bin #7 by the old pole with p-values less than 1×10^{-7} (Figure 5c & 5g). Additionally, a significant decrease at bin # 2 by the new pole was observed in only new mother comparison ($p = 0.007$) (Figure 5g), which may correspond to the steeper slope at the first bin of new mother versus old mother in Figure 4. On the other hand, significant increases at bin #4 and #5 were observed in both new mothers ($p < 1 \times 10^{-7}$, $< 1 \times 10^{-7}$) and old mothers ($p < 1 \times 10^{-7}$, $= 1.85 \times 10^{-4}$, respectively) from birth to division (Figure 5c & 5g). By dividing the transect into smaller sections, here 8 bins compared to 4-bin analysis in Figure 4, we were able to pinpoint more precisely and confirm that ribosome may be shuffled from the old pole to the mid-section of a mother as she was preceding towards division. The increases in the mid-section were again more drastic at the area where the new pole for the new daughter is produced. This is more noticeable in old mother at division, as her incoming daughters are born with a higher asymmetry, favoring new daughter. To discover whether ribosome distribution at division in the mother will be translated into her daughters at birth, we then did a comparison across generation.

Mothers at division (Figure 5c & 5g) were cut in half based on the lengths of daughter pairs, and renormalized in length into 4 bins and fluorescence to compared with newborn daughters. In the comparison between old mother halves and her daughters, we found significant increases at bin #1 (new pole) of both new and old daughters at birth compared to bin #4 and #5 (mid-section) of old mother at division ($p = 0.003$, 0.001, respectively) (Figure 5d). Making up the increases at bin #1, florescence at all three other bins in both daughters decreased, although no significance was associated. However, this implies that another ribosome shuffling event happened between division of the old mother and birth of her daughters, favoring the new poles

of the daughters. In the comparisons done with new mother lineage, fluorescence distribution along transect of new daughter at birth was observed to have no difference compared to new half of her mother at division. On the other hand, old daughter experienced a significant decrease at bin #3 ($p = 0.024$) by the old pole accompanied by a significant increase at bin #1 ($p = 0.012$) by the new pole, compared to bin #7 (old pole) and bin #5 (mid-section) of new mother at division (Figure 5h). Old daughter from a new mother appeared to also shuffle ribosome to the new pole during the time between division of mother and birth of daughter. However, this shuffling event did not happen in new daughter from a new mother, which may be explained by the fact that she was the newest daughter among the four. In other words, in the preparation of distributing ribosomes by a mother at division, only new mother would arrange ribosome somewhat perfectly at the new pole, in a way that her new daughter would benefit from saving the energy to further shuffle ribosome at birth.

At the end, fluorescence distribution of old and new daughters at birth were compared to their mothers at birth one generation backwards. No significant difference was found, which suggests a complete cycle in the ribosome dynamics within and across generations (Figure 5d & 5h).

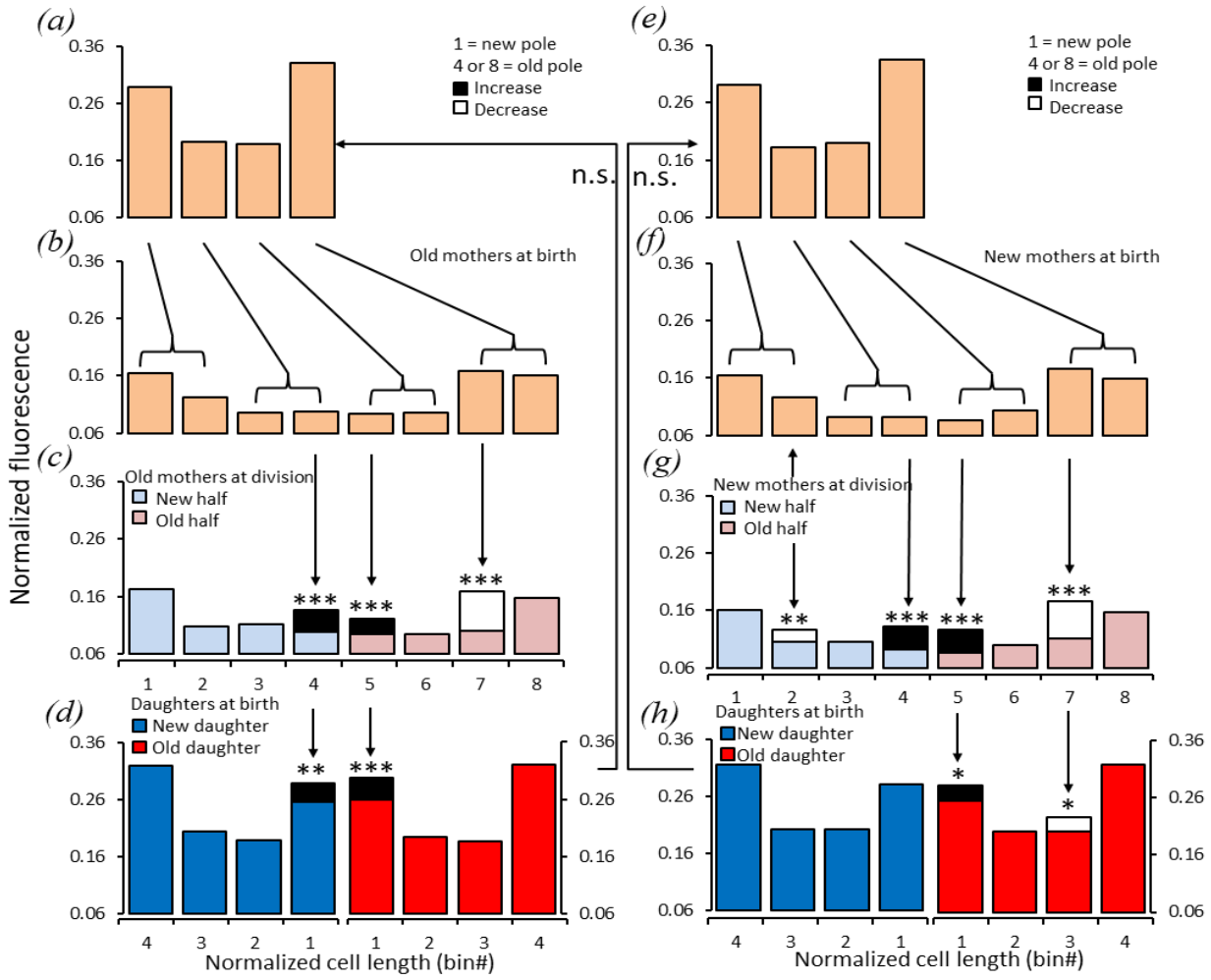

Figure 5. A complete cycle of fluorescence distribution along transects in mothers of trios from birth to division, and to their daughters at birth. Note only changes that are significant are shown. (a) Old mothers at birth with normalized transect length of 4 bins (b) Old mothers in (a) renormalized to 8 bins. (c) Changes in florescence from old mothers at birth to division. Mothers at division show a lower normalized fluorescence at bin #7 ($p < 1 \times 10^{-7}$) and higher at bin #4 and #5 ($p < 1 \times 10^{-7}$, 1.85×10^{-4} , respectively). (d) Fluorescence changes from new and old halves of old mothers at division to respective daughters at birth. Note orientations of transect are parallel to mothers at division, with new poles (bin #1) in the middle. Both new and old daughters at birth show higher fluorescence at bin #1 ($p = 0.003$, 0.001, respectively), compared to bin #4 and #5 of old mothers at division. To complete the cycle, fluorescence distribution of old daughters at birth (red) is compared to old mother at birth (a), resulting in no significant difference. (e) New mothers at birth in 4 bins (n = 68 trios). (f) New mothers at birth 8 bins. (g) Fluorescence changes in new mother at division against at birth. Negative changes are at bin #2, #7 ($p = 0.007$, 0, respectively) and positive at bin #4 and #5 ($p < 1 \times 10^{-7}$, $< 1 \times 10^{-7}$, respectively). (h) Fluorescence changes from new and old halves of new mothers to new and old daughters at birth. Old daughters at birth (red) have lower fluorescence at bin #3 ($p = 0.024$) and higher at bin #1 ($p = 0.012$) compared to bin #7 and #5 of mothers old half at division (pink). New daughters at birth are not significant different from new mother at birth (a).

Correlation between ribosomal density and elongation rate of single cells

Because ribosomal levels and growth rates are correlated [15, 16], we also compared the two traits in our single cells. First, we determined that new daughters grew faster than old daughter with a ratio of 1.09 ± 0.011 ($p = 3.9 \times 10^{-16}$). When dividing the daughters into originating from either new or old mothers, the ratio was 1.07 ± 0.011 ($p = 2.8 \times 10^{-7}$) and 1.11 ± 0.017 ($p = 1.3 \times 10^{-10}$), respectively, thereby following the same pattern as ribosomal asymmetry between daughters (Figure 3e). When comparing the single cells' ribosomal content versus elongation rate (both normalized), the correlation was significant both when daughters originated from new ($r = 0.233$, $p = 4 \times 10^{-4}$, n = 198 pairs) and old mothers ($r = 0.387$, $p < 1 \times 10^{-5}$, n = 216 pairs), (Figure 6), thereby confirming earlier data [15, 16]. Noteworthy, the correlation was stronger and showed a larger range between the two daughters when originating from old mothers than from new mothers, acquiring a similar pattern as an earlier report of correlation between levels of expressed proteins and elongation rate in *E. coli* [14].

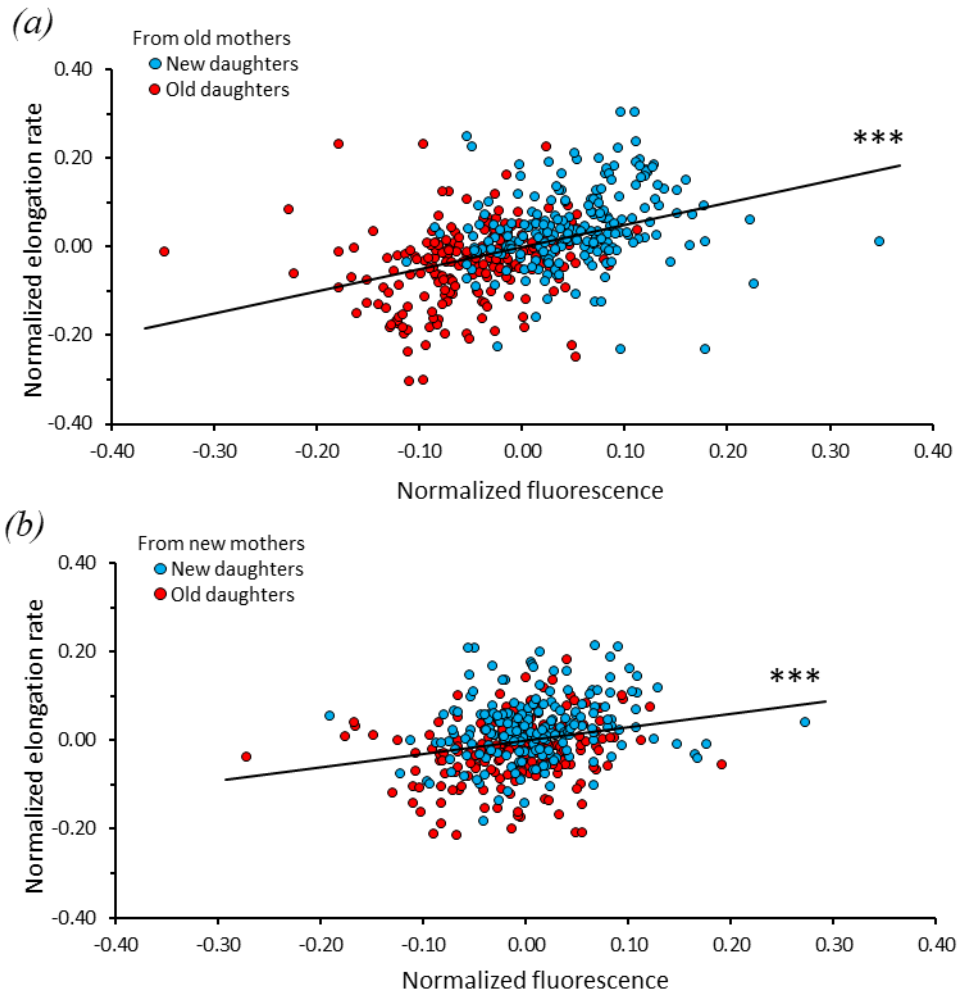

Figure 6. Correlation between normalized YFP fluorescence and normalized elongation rate. Since the normalized data did not conform to a standard Gaussian distribution, statistics and comparisons on correlation were done by randomizing the data to obtain a null distribution of correlations. The reported p-values indicate the probability that the null distribution of correlations contains values that are larger than the observed correlation. (a) Normalized fluorescence versus normalized elongation rate between new and old daughters from old mothers. Correlation r = 0.387, slope = 0.498, $p < 1 \times 10^{-5}$ (***), n = 216 daughter pairs. (b) Normalized fluorescence versus normalized elongation rate between new and old daughters from new mothers. Correlation r = 0.233, slope = 0.301, p = 0.0004 (***), n = 198 daughter pairs. A comparison of observed correlation from old and new mothers (figure 6a versus b) was found to be significant ($p < 2.2 \times 10^{-16}$).

DISCUSSION

Microbial aging in symmetrically dividing cells have slowly been unraveled during the last 15 years [14, 22, 23], showing evolutionary advantages and favoritism of the daughter that inherits the cells´ youngest poles, the new daughter. Since the asymmetrical pattern between the new and the old daughter is part stochastic and part deterministic, a single cell approach is required based on individual cells from birth to division and its generational lineage daughters to single out the deterministic part. Similar to the pattern and reasoning in our earlier study on the levels of expressed gene products [14], our results revealed that also ribosomes, the protein factories of the cells, follow this same asymmetrical pattern with a higher presence in the new pole of mothers at division, and in the new daughter at birth (Figure 3). Interestingly, this asymmetry is higher between poles of old mothers, and between daughters originated from an old mother.

One hypothesis for the ribosomal asymmetry might be space limitation at the old pole of the old daughter. It was previously discovered that aggregates of oxidated and misfolded proteins accumulate more in the old poles and old daughters, compared to new poles and new daughters [7,10]. Therefore, the old mother linage accumulates increasingly more damaged protein aggregates at the old pole, while the new mother linage acquires less damage. Because aggregates take up space at the old pole, ribosomes are hindered to reside at the old pole and ribosomal level was found to be higher at the new pole end. Furthermore, the new mother linage has not yet accumulated damaged aggregates large enough to create space limitation at the old pole, thus, poles of the new mother would have a more similar level of ribosomes than those of the old mother would. Upon division of the mothers, the maternal old pole is allocated to the old daughter (Figure 1) along with the damage proteins. This could then explain the higher

ribosomal level in the new daughters and the more pronounced ribosomal asymmetry between daughters of old mothers.

When spatially following the ribosomal content over a cell's life cycle from birth to division, a decrease was seen at the old pole accompanied by an increase at the mid-section where the two new poles were being produced (Figure 4). This pattern was true for both new and old mothers. Interestingly, the increase at the mid-section was slightly higher on the side facing the mother cell's new pole that will be the new daughter after division, than the side facing the old pole that will become the old daughter. As a more precise comparison, binning the transect into 8 parts revealed a similar pattern. More importantly, this clearly show that the increase of the middle region at division was biased towards the future new daughter and the bias was more noticeable in the old mother (Figure 5). This is consistent with the finding that pole ratio of old mothers at division was significantly larger than 1, which rendered her new pole half more ribosomes (Figure 3). Therefore, we could conclude that from birth to division of a mother, there was a shuffling of ribosomes from the old pole to the middle section, favoring what will become the new daughter, consequently dis-favoring the old daughter.

A possible contribution to the shuffling of ribosomes could be the movement of nucleoid. Because distribution of nucleoid anti-correlates with that of the ribosome inside a cell [3] and nucleoid does not reach to the old pole of a daughter cell at birth [26], relatively more ribosomes will be allocated to the old pole end of a cell. As a cell grows, nucleoid will elongate and reach the old pole, which could be why we observed a significant decrease in ribosomes at the old pole end.

By following cells across generation from the division of mothers to the birth of their daughters, we found that the pole ratios of the mothers were translated into their daughter ratios

(Figure 3), which implies that a mother at division has internal control in the allocation of ribosome between her two polar halves and thus her two daughters. Interestingly, this internal control may allow a mother to create bias or asymmetry between her daughters. Despite pole ratios were translated into daughter ratios, differences were found in the analyses using transects, which show significant increases at the new poles of daughters from old mothers (Figure 5d) and at new pole of old daughters from new mothers accompanied by significant decreases near their old pole (Figure 5h).

Out of the four daughters, only new daughters from new mothers, which were most free of damaged protein aggregates, received ribosomal distributions that were the same as the mother half at division. This scenario may be linked to the evolutionary advantage that the new mother cells gave to the new daughter by saving her energy to reconstruct or relocate ribosomes at the time of birth. Despite this being a tempting explanation, there were a few drawbacks in the comparison between a mother cell at division and her daughters. In the data collected, daughter cells at birth were not born in the same length. Even with cutting the mother cell in half based on the length of daughters at birth, we may not be able to precisely locate the division plane, which then made parallel comparison less accurate. Furthermore, transect may not be the best representative ribosomal profile for a cell, because information could be lost if ribosomes were located outside the long axis of the cell. For future experiments, it is highly suggested to cut a cell vertically along the long axis into slices, which can retain all information within the cell.

Because intracellular ribosomal levels and growth rates are positively correlated [15, 16, 18, 24], it follows that the new daughters from old mothers, with its higher ribosomal content than its older sibling, should demonstrate a faster growth. Our results showed this being true with a positive single cell correlation between elongation rate and ribosomal content (Figure 6). The

correlation was both higher, stronger and showed a larger range of variation when the daughters originated from old mothers than from new mothers. These results confirm both the reliability of the method and additionally strengthen the result in our earlier study correlating protein levels as expressed gene products with higher elongation rates in new daughters compared to their older sibling from old mothers [14]. It is also consistent with mothers allocating more of the damaged proteins to her old daughter and rendering the old daughter a slower growth rate [5, 7, 10].

Combined with earlier studies, our results further show that the new daughter is given an evolutionary advantage compared to her older sibling. Such deterministic asymmetric division of advantageous (ribosomes) and disadvantageous (aggregates) can be argued to be the earliest form and the origin of aging. Aging could therefore be argued to go as far back in time to bacteria, the earliest known form of cellular life.

This thesis, in part, is currently being prepared for submission for publication of the material: Chao, Lin; Chan, Chun (first co-author); Shi, Chao; Rang, Ulla Camilla. "Spatiotemporal Allocation of Ribosomes to Daughter Cells is Determined by the Age of the Mother in Single *Escherichia coli*" *In preparation*. The thesis author was the primary investigator and author of this material.

REFERENCE

[1] Robinow, C., & Kellenberger, E. (1994). The bacterial nucleoid revisited. *Microbiological Reviews*, *58*(2), 211–232.

[2] Nielsen, H. J., Ottesen, J. R., Youngren, B., Austin, S. J., & Hansen, F. G. (2006). The*escherichia coli*chromosome is organized with the left and right chromosome arms in separate cell halves. *Molecular Microbiology*, *62*(2), 331–338.

[3] Bakshi, S., Siryaporn, A., Goulian, M., & Weisshaar, J. C. (2012). Superresolution imaging of ribosomes and RNA polymerase in live escherichia coli cells. *Molecular Microbiology*, *85*(1), 21–38.

[4] Stewart, E. J., Madden, R., Paul, G., & Taddei, F. (2005). Aging and death in an organism that reproduces by morphologically symmetric division. *PLoS Biology*, *3*(2).

[5] Proenca, A. M., Rang, C. U., Qiu, A., Shi, C., & Chao, L. (2019). Cell aging preserves cellular immortality in the presence of lethal levels of damage. *PLOS Biology*, *17*(5).

[6] Rang, C. U., Peng, A. Y., & Chao, L. (2011). Temporal Dynamics of Bacterial Aging and Rejuvenation. *Current Biology*, *21*(21), 1813–1816.

[7] Rang, C. U., Proenca, A., Buetz, C., Shi, C., & Chao, L. (2018). Minicells as a damage disposal mechanism in escherichia coli. *MSphere*, *3*(5).

[8] Rang, C. U., Peng, A. Y., Poon, A. F., & Chao, L. (2012). Ageing in escherichia coli requires damage by an extrinsic agent. *Microbiology*, *158*(6), 1553–1559.

[9] Chao, L. (2010). A model for damage load and its implications for the evolution of bacterial aging. *PLoS Genetics*, *6*(8).

[10] Lindner, A. B., Madden, R., Demarez, A., Stewart, E. J., & Taddei, F. (2008). Asymmetric segregation of protein aggregates is associated with cellular aging and rejuvenation. *Proceedings of the National Academy of Sciences*, *105*(8), 3076–3081.

[11] Łapińska, U., Glover, G., Capilla-Lasheras, P., Young, A. J., & Pagliara, S. (2019). Bacterial ageing in the absence of external stressors. *Philosophical Transactions of the Royal Society B: Biological Sciences*, *374*(1786), 20180442.

[12] Proenca, A. M., Rang, C. U., Buetz, C., Shi, C., & Chao, L. (2018). Age structure landscapes emerge from the equilibrium between aging and rejuvenation in bacterial populations. *Nature Communications*, *9*(1).

[13] O'Connor, O. M., Alnahhas, R. N., Lugagne, J.-B., & Dunlop, M. J. (2022). Delta 2.0: A deep learning pipeline for quantifying single-cell spatial and temporal dynamics. *PLOS Computational Biology*, *18*(1).

[14] Shi, C., Chao, L., Proenca, A. M., Qiu, A., Chao, J., & Rang, C. U. (2020). Allocation of gene products to daughter cells is determined by the age of the mother in single *escherichia coli* cells. *Proceedings of the Royal Society B: Biological Sciences*, *287*(1926), 20200569.

[15] Schaechter, M., MaalOe, O., & Kjeldgaard, N. O. (1958). Dependency on medium and temperature of cell size and chemical composition during balanced growth of salmonella typhimurium. *Journal of General Microbiology*, *19*(3), 592–606.

[16] Kjeldgaard, N. O., & Kurland, C. G. (1963). The distribution of soluble and ribosomal RNA as a function of growth rate. *Journal of Molecular Biology*, *6*(4), 341–348.

[17] Neidhardt, F. C., & Magasanik, B. (1960). Studies on the role of ribonucleic acid in the growth of bacteria. *Biochimica Et Biophysica Acta*, *42*, 99–116.

[18] Poulsen, L. K., Licht, T. R., Rang, C., Krogfelt, K. A., & Molin, S. (1995). Physiological state of escherichia coli BJ4 growing in the large intestines of streptomycin-treated mice. *Journal of Bacteriology*, *177*(20), 5840–5845.

[19] Chao, L., Rang, C. U., Proenca, A. M., & Chao, J. U. (2016). Asymmetrical damage partitioning in bacteria: A model for the evolution of stochasticity, determinism, and genetic assimilation. *PLOS Computational Biology*, *12*(1).

[20] Łapińska, U., Glover, G., Capilla-Lasheras, P., Young, A. J., & Pagliara, S. (2019). Bacterial ageing in the absence of external stressors. *Philosophical Transactions of the Royal Society B: Biological Sciences*, *374*(1786), 20180442.

[21] Yang, Y., Santos, A. L., Xu, L., Lotton, C., Taddei, F., & Lindner, A. B. (2019). Temporal scaling of aging as an adaptive strategy of *escherichia coli*. *Science Advances*, *5*(5).

[22] Florea, M. (2017). Aging and immortality in unicellular species. *Mechanisms of Ageing and Development*, *167*, 5–15.

[23] Moger-Reischer, R. Z., & Lennon, J. T. (2019). Microbial Ageing and Longevity. *Nature Reviews Microbiology*, *17*(11), 679–690.

[24] Rang, C. U., Licht, T. R., Midtvedt, T., Conway, P. L., Chao, L., Krogfelt, K. A., Cohen, P. S., & Molin, S. (1999). Estimation of growth rates of *escherichia coli* BJ4 in streptomycin-treated and previously germfree mice by in situ rrna hybridization. *Clinical Diagnostic Laboratory Immunology*, *6*(3), 434–436.

[25] Miller, J. H. (1972, January 1). *Experiments in molecular genetics (1972 edition)*. Open Library. Retrieved May 17, 2022.

[26] Fisher, J. K., Bourniquel, A., Witz, G., Weiner, B., Prentiss, M., & Kleckner, N. (2013). Four-dimensional imaging of E. coli nucleoid organization and dynamics in Living Cells. *Cell*, *153*(4), 882–895.